

THE CHALK RIVER SUPERCONDUCTING CYCLOTRON

J.H. Ormrod, C.B. Bigham, E.A. Heighway, J.D. Hepburn, C.R. Hoffmann, J.A. Hulbert and H.R. Schneider
 Atomic Energy of Canada Limited, Research Company
 Chalk River Nuclear Laboratories
 Chalk River, Ontario, Canada K0J 1J0

Summary

The Chalk River four-sector, K=520 superconducting cyclotron in combination with its 13 MV tandem Van de Graaff injector is designed to accelerate all ions from lithium (to 50 MeV/u) to uranium (to 10 MeV/u). After extended testing of the magnet, radiofrequency accelerating system and other sub-systems, the cyclotron is being moved from the development laboratory to the new addition to the tandem building. Recent development work is reviewed and the current status of the various cyclotron sub-systems is given.

Introduction

The Chalk River heavy-ion accelerator facility is shown in Fig. 1. Ions from a negative ion source are preaccelerated to 300 keV and velocity modulated by a buncher before injection into the tandem Van de Graaff accelerator. The buncher produces a time focus at the tandem terminal to minimize longitudinal phase-space dilution from the stripper. The dispersion from the first bending magnet downstream from the tandem is used for energy stabilization and charge-state selection. The beam is injected into the cyclotron along the midplane and intercepted by a carbon stripper foil near the cyclotron center. A rebuncher between the tandem and the cyclotron again produces a time focus at this foil. Four dees operate up to 100 kV peak and accelerate the beam to a radius of 650 mm where the beam is electrostatically deflected into a magnetic channel composed of iron bars and superconducting windings. Use of superconducting windings allow adjustable steering and radial focusing in the channel. A conventional beam transport system beyond the cyclotron guides the beam to the various target locations.¹ Initial operation of the superconducting magnet,¹ detailed magnetic field mapping,² out-of-magnet radiofrequency testing,³ the extraction system⁴ and the bunching system⁵ have been previously described.

Calculations

There have been two main computation efforts in preparation for commissioning the cyclotron. The first has been to improve the static and dynamic orbit codes to ease the commissioning by combining in one code all the features previously handled separately; injection, including automatic matching and second order transfer matrix calculations needed for beam transport tune-up, perturbation field handling and detailed treatment of the extraction system with automatic threading of the beam through the deflector and magnetic channels. The second effort has been to refine the calculations of the magnetic field in the coil region beyond the range of the main field measuring apparatus and include the perturbing effects of the holes in the yoke walls. These perturbations have been calculated using a current sheet representation for the magnetization in the steel but empirically normalized as a function of field intensity to measurements along the injection path. Now, the parameters for a new ion can be quickly calculated and the beam progress from outside the cyclotron through injection, acceleration and extraction to the cyclotron exit readily modeled.

Cryogenics

Three chosen design features of the Chalk River superconducting cyclotron result in a relatively large refrigeration load at the main coil cold box at 4.5 K. These features are the high coil current (2300 amperes maximum) which reduces coil voltages by giving a lower inductance, the non-magnetic cryostat wall which eases cryostat centering requirements but forces small clearances between the poles and the magnet coil, and the use of a superconducting extraction channel. In addition the midplane cryopumps are filled from the main coil helium can.

The CTI 1400 liquefier was able to keep the cryostat cold continuously for 18 months during the last development run, but was not considered adequate to provide cooling for the whole system without interruption for 24 hours per day. Therefore a larger capacity liquefier, a Koch 2800HR, has been installed in the nearly-completed cyclotron laboratory. This machine will supply 90 litres of liquid helium per hour or 52 litres per hour without liquid nitrogen precooling. Its output can be increased to 120 litres per hour by adding an extra compressor. It is anticipated that it will be possible to operate with little or no liquid nitrogen precooling because the boiloff rate for the whole system is expected to be no more than 47 litres per hour.

The liquefier contains redundancy for maintenance in that there are two independent sets of engines and five separate compressors. Loss of one component can be made up by increasing liquid nitrogen precooling and by drawing on the 1000 litre liquid helium buffer reservoir.

A new set of refrigerant transfer lines is under construction for the operational system. All the lines are flexible so that they can be manufactured straight and not bent until installation. This allows optimization of the superinsulation wrapping and eases assembly, maintenance and repair. It has also made

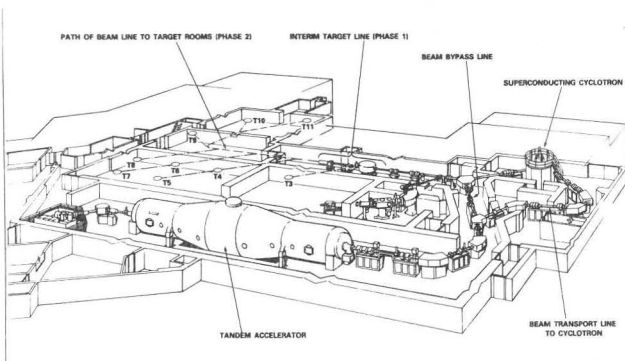


Fig. 1 View of the heavy-ion accelerating facility.

We are now in the final year of phase 1 funding, approved in 1980, that includes the building additions and all equipment (shown detailed in Fig. 1) needed to transport the beam to the beam hall beyond the cyclotron vault. Phase 2 funding will provide some new equipment and the remainder of the beam transport elements needed to guide the beam to the remaining target rooms (trajectories shown as dashed lines in Fig. 1).

possible the inclusion of 100 K thermal shielding to the greater part of the line length reducing overall system loss and the gas circulation burden. Figure 2 shows one of the new transfer lines.

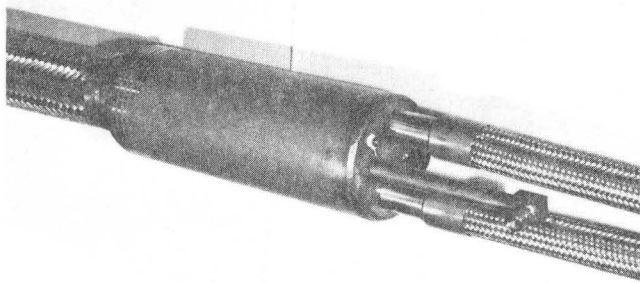


Fig. 2 One of the three main transfer lines showing the transition from the thermally shielded section (on the left) to the divided ends which connect to the main magnet cryostat. The shielded section has a length of 6 metres.

Cooling of the extraction channel modules located in the midplane gap between the main magnet coils poses a mechanical design challenge because of the small clearances between warm and cold surfaces. Near the beam inlet to the channel, the insulation between cryostat wall and channel helium vessel is limited by a gap of between 2 and 3 mm. Here layers of aluminized mylar and fine dacron mesh (bridal veil) will be used, with a copper foil interleaved thermal shield. The channel beam pipe is cooled with helium gas at 100 K to provide both a thermal shield for the channel bore and a thermal sink for the energy of spilled ions from the beam. The ends of the channel beam pipe are attached to the inlet and exit ports by metal bellows which take up misalignment before cooling and thermally isolate the cold beam pipe from the warm ports. The channel is cooled by liquid helium, gravity fed from the lower main coil helium vessel and boiloff gas from the channel is returned to the top of the upper main coil vessel where it mixes with the boiloff from the main coil.

Vacuum System

The cyclotron has three separate vacuum systems - the cryostat vacuum, the midplane vacuum and a coarse vacuum on the pole side of the 3 mm thick copper liners that cover the poles (see Fig. 3). These liners are protected from differential pressures by "pop-valves" between the coarse and midplane vacuums that open at 10 kPa and by a 100 L/s turbomolecular pump that evacuates the midplane and exhausts into the coarse vacuum pumping line. This pump cannot support a significant vacuum differential. Coarse vacuum pressures in the 0.1 Pa range are typical.

In addition to the 100 L/s turbopump, high speed pumping at the midplane is provided by two cryopanel situated in upper magnetic valleys where they make a small but noticeable contribution to the dee-to-ground capacitance. The cryopanel are located in a weaker region of the midplane rf field but are nevertheless in quite a strong field. Figure 4 shows the cryopanel components before assembly.

The cryopanel are cooled by direct liquid helium transfer from the main magnet coil vessel. The helium consumption is low enough that the intermittent transfer causes negligible perturbation on the coil coolant level. Both cryopanel are filled automati-

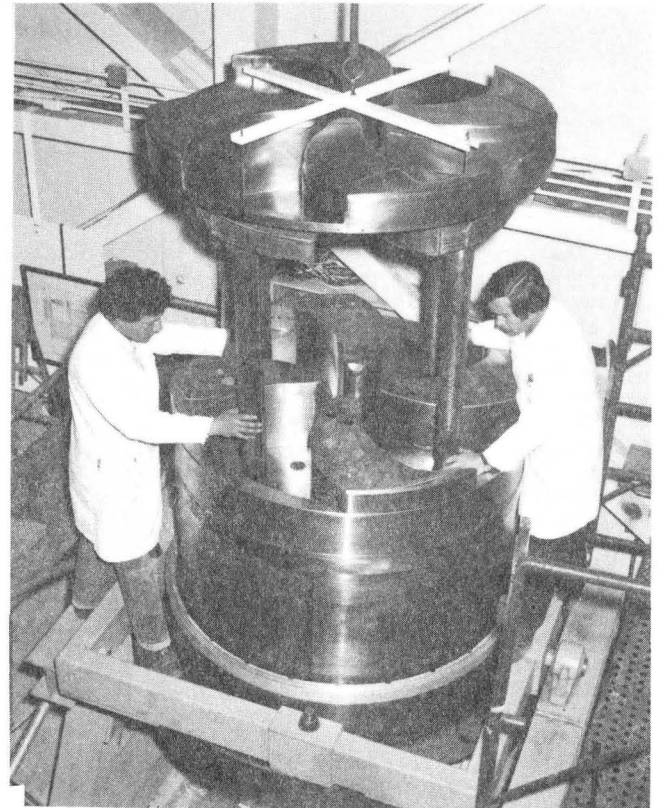


Fig. 3 The copper liner being installed on the upper pole.

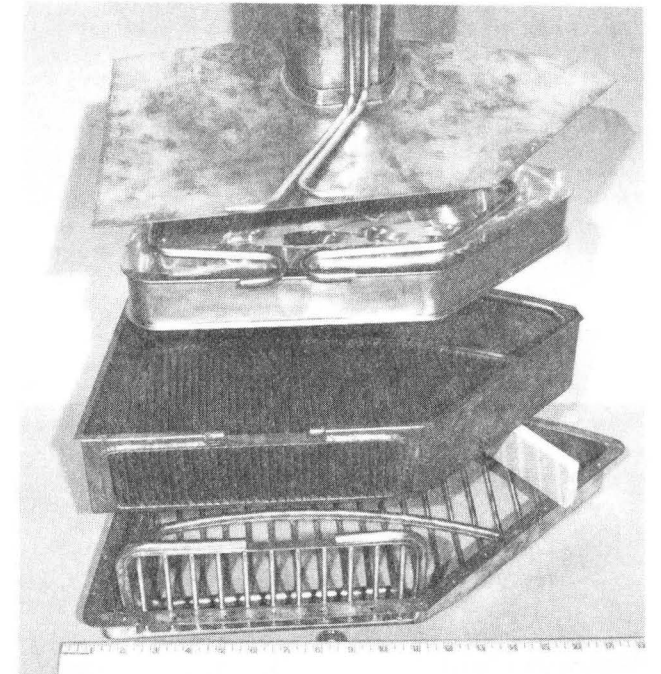


Fig. 4 1500 L/s cryopanel.

cally through their own transfer lines in response to signals from thermometric level sensors. Thermal shielding for each cryopanel and the liquid transfer line is provided solely by the cold boiloff gas. The developmental cryopanel operated with 80% of full rf voltage in the midplane cavity with a liquid boiloff of less than 1 litre per hour and a pumping speed of 1500 litres per second for air. This performance was achieved by careful design and testing of the radiation-rf baffles. The purpose of the outer water

cooled baffle is purely to attenuate rf while providing a large pumping aperture. The inner gas-cooled baffle is a more conventional chevron type. At present, the condensation surface (4.4 K) is a flat stainless steel plate but could be coated with adsorbing material should enhanced hydrogen trapping be found to be necessary. Reactivation and purging of the panel surface is carried out by circulating warm helium gas through the panel reservoir.

During development, interruption of the water flow in the outer baffle resulted in a frozen pipe which burst and subsequently flooded the midplane. To prevent this recurring, the water is purged automatically with an air blast if the flow stops, or the rf is switched off, or the midplane vacuum pressure rises. In addition, the production cryopanels are fitted with trace heaters along the water lines.

Cyclotron Magnet

After the vacuum and radiofrequency tests in the magnet were completed in the development laboratory, the magnet was dismantled and the steel reassembled in the new addition to the heavy-ion laboratory. The coarse vacuum system piping was rebuilt to conform to the new laboratory layout and other services have been installed. The upper trim rod drive system has been installed and successfully operated under computer control; the lower trim rod drive system will not be installed until the magnet realignment has been confirmed with the field measuring apparatus. Figure 5 shows the assembled magnet in the new laboratory.

A ground fault between the main coil and its stainless steel container occurred again and because of its location it was suspected and later confirmed to be similar to the short circuit experienced previously² - an accumulation of slightly magnetic debris near the midplane of the upper coil. The short circuit was removed by passing a 6 A current through it, with the current split in opposite directions between both inner coils to minimize stored energy. The cryostat has been opened for installation of the extraction channel giving access to the holes through which the short was cleared previously. The plugs were extracted and the same tool used to remove the fragments of magnetic material. This time, despite many more magnet on-off cycles only 36 mg of material were collected, compared to 140 mg last time and we believe most of the offending material has been removed.

The installation of the magnetic channel in the cryostat is scheduled for early summer and a special jig has been fabricated to transport the cryostat to the new laboratory for installation in the magnet.

Radiofrequency Structure and Controls

The radiofrequency accelerating structure was set up initially in a dummy vacuum vessel so that high power testing could be carried out separately from the magnet development³. Although full voltage was reached for short periods in early tests, a major effort was required to develop reliable sliding short tuner contacts⁶. Tests were run over the full frequency range up to 80-90 kV including a "24-hour" demonstration run at 32 MHz in the 0-mode. The temperatures at the monitored points throughout the structure remained stable and maintenance of good vacuum indicated that there were no hot-spots. Dummy cryostat wall temperatures were higher in the π -mode than 0-mode but stabilized at a reasonable level. The actual cryostat has better cooling and should have smaller temperature increases.

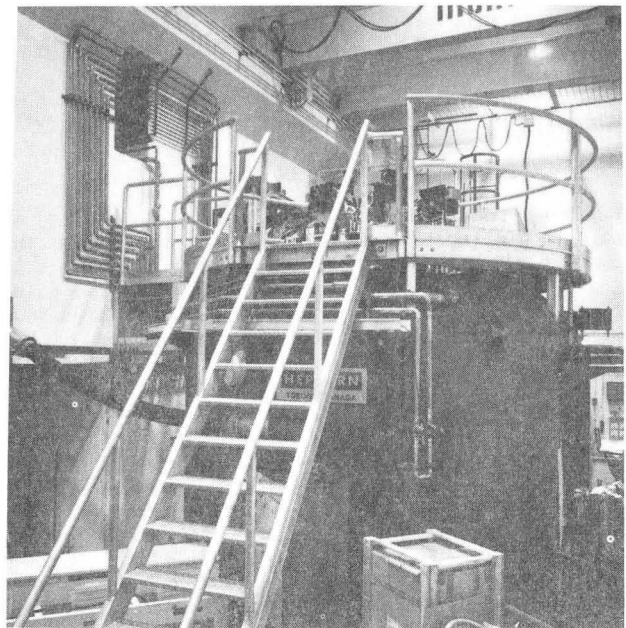


Fig. 5 Cyclotron magnet in heavy-ion laboratory. The aperture in the wall in the upper left hand corner of the photograph gives access to the service room for helium transfer lines.

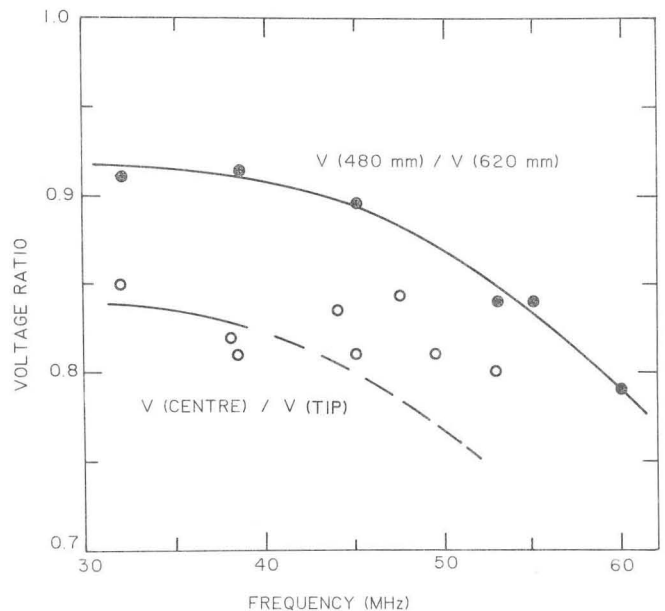


Fig. 6 Radial variation of dee voltage.

The dee voltages were measured using an intrinsic germanium γ -ray spectrometer to measure the end-point x-ray energy produced by electrons crossing the dee gap in the structure. Electron guns were installed at radii of 620 mm (dee tip), 480 mm and the injection radius of 150 mm to obtain measurements at specific points in the structure. Well defined end points were obtained at 480 mm and 620 mm by subtracting gun-off from gun-on spectra but the gun at the 150 mm radius did not produce an observable effect. The ratio of voltages at 480 mm relative to voltages at the dee tip as a function of frequency is shown in Fig. 6. It was found that a good measure of the dee tip voltage could be obtained by using a collimator on the spectrometer arranged to see only the dee tip "hot-spot" and this was used for voltage calibration after the guns were removed. During π -mode operation, a high energy spectrum was observed from the central region. At 32

and 38 MHz, this spectrum had a well defined edge and is believed to give a good measure of the resonator-to-resonator voltage, i.e., twice the dee voltage. At higher frequencies the edges are not as sharp and seem to be at too high an energy. For this essentially quarter wave resonator, the ratio at higher frequencies is expected to be like the dashed line.

After completion of the tests in the dummy vessel, the structure was installed in the magnet for tests with magnetic field. The copper liners, or ground planes, of the rf structure were designed to be a close fit to the flutter poles (see Fig. 3). However, corrections to the magnetic field required the addition of shims to the inner and outer regions of the pole faces and reforming of the liner was required to fit over these shims.

The difficult joint between the outer conductor of the tuner and the liner failed several times. It has an O-ring vacuum seal behind an rf gasket. It was refitted carefully on the pole and temperature probes repositioned near the joint from less critical regions of the liner. During the rf tests it became apparent that the cooling of the joint was not good enough. This was aggravated by the fact that the cooling water pressure was low because of inadequacies in the temporary piping from the cooling system. The in-magnet tests were then restricted to 80 kV to protect this joint. After the tests, the joint was refitted and some conduction cooling pads added so that with the correct water pressure, the joint should be capable of full power operation.

After installation of the rf structure in the magnet had been completed, commissioning experiments were carried out over most of the rf frequency range at magnetic inductions between 2 and 5 T. Electron loading effects were different from the low level multipactoring observed with no magnetic field and complicate the initial "turn-on" but did not limit the range of operation.

Initially, a 300 L/s cryopanel was used in these tests and pressures in the high vacuum region of the structure were similar to those observed in the dummy vessel experiments using the same cryopanel. Initial pressures were in the low 10^{-3} Pa range and after a few hours dropped to the 10^{-4} Pa range. With rf on, the pressure increased 2 to 4 times initially and then decreased towards the level obtained with the rf off. Operating periods were not long enough to obtain a good indication of the ultimate levels. When the 1500 L/s cryopanel was installed, the vacuum improved and tests were run at 32 MHz to 80 kV, at 49 MHz to 65 kV and at 60 MHz to 60 kV with magnetic inductions between 2.2 and 5 T. Electron loading effects at first turn-on were not very different with the improved vacuum but conditioning was much easier.

The temperature of the cryostat wall copper inserts, which complete the rf cavity between the liners on the poles, was monitored during rf operation. As expected, the temperature increases are small in the 0-mode and larger in the π -mode. The cooling in the "valleys" was adequate but the temperature rise in the "hills" was too high during long π -mode runs. This may be caused by insufficient copper plating thickness on the cryostat wall or by resistive heating of temporary steel flanges on the probe holes. Existing plating will be thickened and any exposed steel surfaces heavily copper plated.

The voltage and phase stability of the dee was measured. The voltage stability is better than 0.1% (the limit of the measurement). The one minute phase

drift was 0.2° or less. There was an approximately 30 Hz component 0.2° in amplitude that may have been mechanical in origin. These stability levels are adequate for initial cyclotron operation.

After the tests in the magnet, the liner-outer conductor joints were refitted and cooling improved. The liners were then reinstalled on the poles before the magnet yoke and poles were moved to the new laboratory.

The control system has been rebuilt and the computer interfacing completed. The power amplifier has been installed in the final location and is being commissioned.

Bunchers

The low energy buncher has changed significantly since last reported⁵. The design as originally conceived included two coaxial independently capacitively loaded resonators driven by a single broad band amplifier. This coaxial design was compact and potentially simple to operate. However, while it performed well over the entire operating range for the fundamental resonance, the design voltage for the second harmonic resonance was only achieved over the bottom two thirds of the operating range in spite of much modeling effort using SUPERFISH and extensive modifications. The coaxial design has been replaced by an opposed resonator design shown in Fig. 7. The new design has switched from rotating vane capacitors to commercial linear vacuum capacitors eliminating a sensitivity to microphonic noise.

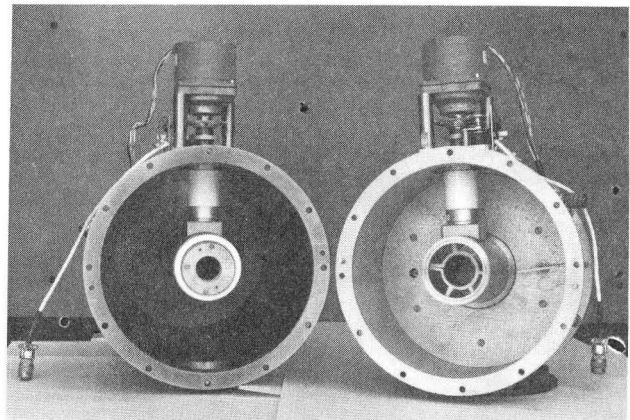


Fig. 7 Low energy buncher.

The single power amplifier has been replaced by two separate power amplifiers. The added expense of this choice is more than offset by the reduction in complexity of the control system. The two amplifier drive uses two fixed coupling loops tuned for critical coupling at the low frequency (higher power) end of the operating range. The use of the single amplifier required the design of a single hybrid coupling loop with two degrees of freedom allowing, but also requiring, tuning of the coupling to both resonances over the entire operating range.

The new buncher has now been vacuum tested and has demonstrated extremely stable, microphonic-free operation showing no sign of multipactoring. It has been successfully operated to design voltage (achieved by approximately 50 Watts into each of the two resonators) over the entire frequency range of 31 to 62 MHz and 62 to 124 MHz respectively. The design voltages, measured by accelerating electrons across the single gridded accelerating gap, of 2 kV and 600 V peak respectively have been easily achieved. Emphasis

has now turned to completing the computer control for the bunchers.

The high energy buncher⁷ structure is a 65 mm drift tube on a sliding short tuned resonator operating up to 20 kV over the 62 to 190 MHz frequency range. A reasonable match to $\beta\lambda$ values is obtained with the 65 mm drift tube by operating the buncher at the 2nd harmonic of the rf frequency for cyclotron harmonics 4 and 6 and at the 4th harmonic for cyclotron harmonic 2. The buncher has been fabricated and testing has started. The tuning range was checked and the shunt impedance measured to obtain the amplifier power rating required - 250-300 W. In the first tests (up to 50 W), it was found that multipactoring was enhanced by ions from the sputter ion vacuum pump. However, with a pulsing circuit to provide a fast turn-on, the buncher can be operated over the entire range.

The phase control of the radiofrequency system is shown schematically in Fig. 8. The signal from the synthesizer is divided into four individually phase controlled lines. The phases must be set so that the bunches formed by the low energy buncher (LEB) pass through the rebuncher (HEB) at the correct phase and also arrive at the cyclotron at the correct phase. The circuit shows that the cyclotron dees are set relative to the HEB. The HEB has a local phase stabilization loop to correct for instabilities in the amplifier and resonator.

It is expected that transit times through the Tandem may vary sufficiently that an active phase feedback to the LEB from the beam bunches may be required. The bunch phase is sensed by an energy analyzer after the HEB, and the slit currents are used to stabilize the phase of the LEB as indicated in Fig. 8.

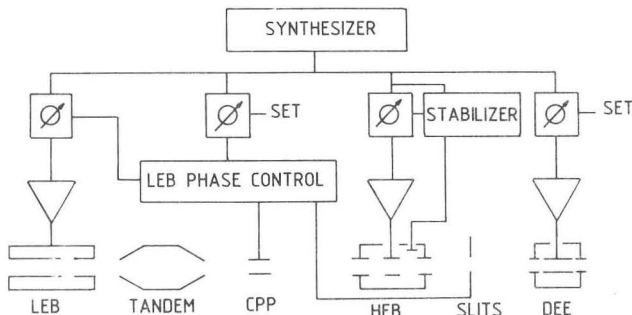


Fig. 8 Schematic of phase control system.

However, the HEB operates at 2 or 4 times the cyclotron frequency and following a large transient it could stabilize the beam on the wrong cycle. To avoid this, the beam phase is also sensed by a capacitive phase probe (CPP). A phase comparison between this signal and a reference signal is used to control the LEB phase during transients and to return the beam buncher to the correct HEB cycle.

Extraction System

The basic elements of the extraction system have been previously described⁴. While the major features have not changed, some details have undergone significant revision. Briefly, the system consists of a single electrostatic deflector followed by several magnetic elements. These elements combine magnetically saturated iron bars and/or superconducting windings in assemblies to provide either (a) fixed radial focusing gradients, or (b) variable steering with fixed radial focusing gradients, or (c) variable

steering and variable radial focusing. Prototype structures of the latter two assemblies have been built and tested and are described elsewhere in these proceedings⁸. First harmonic perturbation fields in the acceleration region generated by the iron are compensated with other iron structures mounted on the inner main cryostat wall. The elements containing superconducting coils have the windings arranged to generate small first harmonic perturbations in the acceleration region.

The active magnetic elements are in two separate serial channels. The first channel contains three identical modules (see Fig. 9) which have iron bars to generate a fixed radial focusing gradient and superconducting windings to produce variable steering fields. The second channel consists of six identical modules. Each has two sets of superconducting windings - one for variable steering and one for variable radial focusing. All channel modules are mounted in the main coil cryostat bridge region. A small local helium can surrounds them which isolates the main cryostat vacuum from the liquid helium bath that cools them.

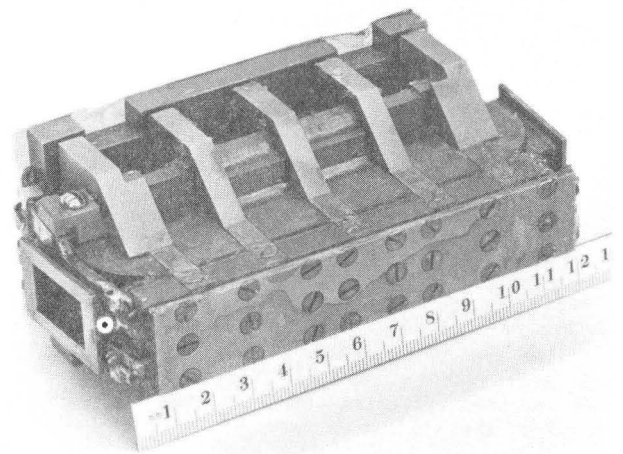


Fig. 9 Channel 1 type module.

Significant revisions made to the superconducting elements include replacement of Nb_3Sn conductor with Nb-Ti, rearrangement of steering winding geometry to use racetrack instead of saddle coils and electrical regrouping of steering windings to form three independent steering groups instead of two. All of the coils in the extraction system will be wound with multifilamentary Nb-Ti having a copper to superconducting ratio of 1.4/1.0 and a critical current of 220 A at a field of 5 T and temperature of 4.2 K. Prototype extraction coils wound with this conductor have achieved short sample critical current. An important mechanical feature of the conductor is that it is flattened in a rolling mill from a circular cross section of diameter 0.5 mm to a rectangular cross section having an aspect ratio of about 3/1. Elongation of the conductor is insignificant and critical current is not affected. Flattening improves winding control and packing fraction and reduces the amount of epoxy present after vacuum impregnation.

The channel modules are being made and tested individually in a superconducting magnet capable of generating background fields up to 5 T. The modules, beam pipe and local helium can will be assembled and mounted in a specially designed cryostat to allow the entire magnetic channel to be tested in its operating configuration at full current but in zero background field before installation in the main coil cryostat.

Probes

For initial cyclotron operation, three probes will be provided. Two of these, located in the mid-plane and separated by 90° move from outside the yoke wall to a radius of 135 mm on straight lines 40 mm offset from the cyclotron center. Interchangeable probe tubes and heads allow radial or axial differential and integral beam measurements. Each probe has an independent vacuum system to allow easy probe changes. The probe vacuum envelope has an edge-welded bellows with 2 m travel as the moving vacuum seal.

The third probe, located just downstream of the electrostatic deflector, has only two positions - withdrawn or fully intercepting the beam. The probe head consists of two plates, each blocking half of the extraction channel aperture to provide radial beam location information.

An LSI-11/23 microcomputer controls the three probes. It collects, analyzes, stores and displays the beam current data and provides communication with the main PDP 11/44 control computer. The displays include a storage oscilloscope, digital and analog-panel meters for currents and digital output for the probe position.

The probes have been built and are in various stages of assembly. Building and programming of the controls is in progress.

Facility Status

Civil construction, including the control room extension, is complete. The installation of special services, such as the closed de-ionized water loop, is nearly complete.

The new negative ion-source cage and low energy analyzing system have been installed and the first beam has been extracted completely under computer control from the new control room.

Broken glass insulators were discovered in some of the struts of the bridge structure that supports the Tandem accelerating column. It was decided to rebuild all of the diagonal members of this structure, so the bridge assembly was completely dismantled and the members shipped to the fabricator. They have been rebuilt and reassembly of the bridge is now in progress. First beam from the Tandem accelerator is scheduled for late this summer.

All of the components for the beam line have been delivered. All of the dipoles and most of the focusing elements have been installed, aligned and tested. The vacuum system and the beam line diagnostic equipment installation are also nearing completion.

The two PDP 11/44 minicomputers have been installed in the new control room and the full complement of CAMAC modules has been purchased and are being installed. System variables are being brought on line as various hardware components are installed.

The cyclotron with all its subsystems is scheduled to be assembled and accelerating its first beam this autumn.

References

1. J.H. Ormrod, C.B. Bigham, K.C. Chan, E.A. Heighway, C.R. Hoffmann, J.A. Hulbert, H.R. Schneider and Q.A. Walker, IEEE Trans. Nucl. Sci., NS-26 (1979) 2034.
2. J.H. Ormrod, C.B. Bigham, E.A. Heighway, C.R. Hoffmann, J.A. Hulbert and H.R. Schneider, Proc. Ninth Int. Conf. Cyclotrons, Caen, France, Editions de Physique (1981) 159.
3. C.B. Bigham, IEEE Trans. Nucl. Sci., NS-26 (1979) 2142.
4. C.R. Hoffmann, Proc. Ninth Int. Conf. Cyclotrons, Caen, France, Editions de Physique (1981) 497.
5. E.A. Heighway, C.B. Bigham, J.E. McGregor, IEEE Proc. NS-30 (1983) 2809.
6. C.B. Bigham, R.J. Burton and J.E. McGregor, these proceedings.
7. C.B. Bigham, A. Perujo, E.A. Heighway and J.E. McGregor, these proceedings.
8. C.R. Hoffmann, J.F. Mouris and D.R. Prouix, these proceedings.